The International Journal of Advanced Manufacturing Technology (2024) 133:2401–2417
https://doi.org/10.1007/s00170-024-13929-6

ORIGINAL ARTICLE

Experimental investigations into the effect of process parameters on the machining quality for ITO conductive glass by using microgroove grinding

Yin Liu[1,2] · Xiaolong Qiu[1,2] · Xingwei Sun[1,2] · Fei Pan[1,2] · Weifeng Zhang[1,2] · Shibo Mu[1,2] · Hongxun Zhao[1,2] · Yadong Gong[3]

Received: 5 December 2023 / Accepted: 27 May 2024 / Published online: 8 June 2024
© The Author(s), under exclusive licence to Springer-Verlag London Ltd., part of Springer Nature 2024

Abstract

To investigate the effect of microscale grinding on the quality of ITO conductive glass, this paper conducted microscale grinding experiments on ITO conductive glass. The influence of process parameters on machining quality was analyzed using microgrinding force, surface roughness, and sheet resistance as indicators. Meanwhile, soda-lime glass was set as the control group to analyze the effect of ITO film. The results indicate that brittle fracture is the main removal method for ITO films, and the glass substrate exhibits two different removal methods, brittle and ductile, depending on the process parameters. The ITO thin film layer suppresses the sheet deformation of the glass substrate, increasing the grinding force and reducing the processing quality. Increasing the spindle speed, reducing the feed speed, and reducing the cutting depth can improve the machining quality. The spindle speed has a significant impact on surface roughness, while the cutting depth has a significant impact on the sheet resistance of the thin film. In addition, soda-lime glass chips mainly appear in powder and granular form, while ITO conductive glass also has flaky thin film chips generated by interlayer fracture.

Keywords ITO conductive glass · Microscale grinding · Material removal mechanism · Processing quality · Grinding chips

1 Introduction

Indium tin oxide (ITO) is a semiconductor thin film material with good conductivity and transparency. After sputtering a layer of ITO thin film on a glass substrate and high-temperature annealing treatment, ITO conductive glass can be obtained. Due to its excellent material properties and mature preparation process, it is widely used in optoelectronic devices, electric thermal conversion, electromagnetic shielding, and other fields [1, 2]. Figure 1 illustrates the specific application scenarios of ITO conductive glass. When this material is applied in precision optoelectronic systems, it needs to have characteristic structures such as microgrooves, microwalls, or micropores at the micrometer level and requires high surface quality and geometric accuracy [3–5]. Microfabrication techniques such as etching and masking based on semiconductor manufacturing processes are costly and inefficient, making it difficult to achieve complex morphology and large depth of field structures. And microscale grinding is formed by the synergistic cutting of microabrasive particles and microedges on the surface of microgrinding wheels to form the machining surface of parts, which has high processing efficiency and is commonly used for the machining of some brittle material microstructures [6].

In order to improve the quality of microscale grinding, some scholars have studied the mechanism of material

✉ Yin Liu
liuyin_neu@163.com

✉ Xingwei Sun
sunxingw@126.com

[1] School of Mechanical Engineering, Shenyang University of Technology, No. 111, Shenliao West Road, Shenyang Economic and Technological Development District, Shenyang 110870, P.R. China

[2] Liaoning Province Key Laboratory of Complex Surface NC Manufacturing Technology, Shenyang University of Technology, Shenyang Economic and Technological Development District, No. 111, Shenliao West Road, Shenyang 110870, P.R. China

[3] School of Mechanical Engineering and Automation, Northeastern University, No. 3-11, Wenhua Road, Heping District, Shenyang 110819, P.R. China

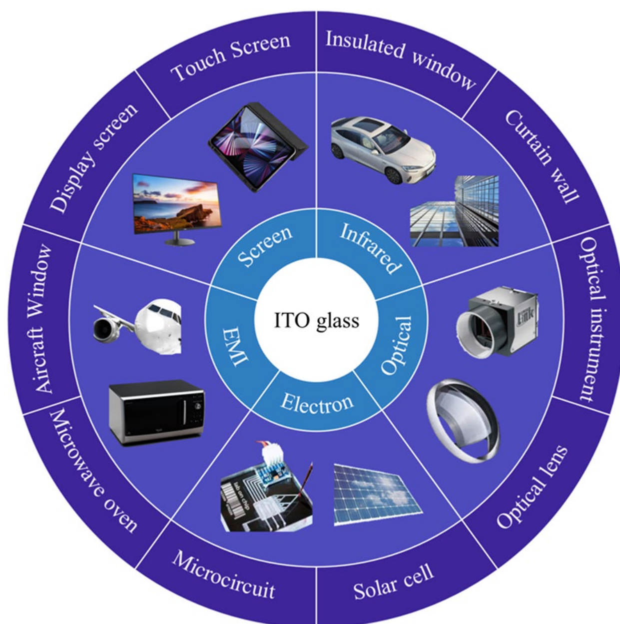

Fig. 1 Application of ITO conductive glass

removal in microgrinding. Perveen et al. [7] conducted microgrinding experiments on BK7 glass using vertical PCD tools. By analyzing the cutting forces and surface roughness under different processing parameters, a prediction model for microgrinding quality was obtained. Cheng et al. [8–10] studied the removal mechanism of brittle materials through microgrinding experiments on hard and brittle materials. Taking into account size effects, abrasive particle distribution, and tool morphology, a theory of maximum undeformed cutting thickness for microscale grinding was proposed based on traditional grinding techniques. Feng et al. [11] used cohesive force method to simulate fracture mode and coupled abrasive trajectory, analyzed surface generation under ductile mode, and successfully predicted the grinding force and surface quality of ceramic materials in microgrinding processing. Ren et al. [3] conducted side microgrinding experiments on monocrystalline silicon, evaluating the quality of microgrinding by surface roughness and average edge collapse width. They analyzed the effects of different microgrinding tools and process parameters on microgrinding quality. Manea et al. [12] conducted a study on microgrinding of K9 glass, analyzing the grinding force component and grinding path based on the critical depths of plowing, sliding friction, and brittle tearing. They established an arithmetic model of grinding force based on the geometric model of abrasive particles and finally verified the reliability of the model through experimental results.

ITO conductive glass is a composite material of brittle film/brittle substrate, and different forms of damage will occur between the thin film layer and the substrate during the processing. For the surface processing of brittle hard coating materials, Kubohori et al. [13] used diamond grinding wheels to grind the Al_2O_3-TiO_2 coating and found that the surface roughness increased with increasing cutting depth and decreased with increasing abrasive particle size. The peeling and detachment of coatings during processing make it difficult to obtain an ideal machining surface, but the higher the TiO_2 content in the coating, the lower the occurrence rate of peeling and detachment. Katahira et al. [14] proposed a high surface quality machining method for titanium nitride-based coatings, which achieves a high-quality surface layer and higher residual compressive stress on the machined surface through specific precision grinding processes. Masoumi et al. [15] studied the grinding force, specific energy, and material removal mechanism during surface grinding of HVOF-sprayed coating and found that an increase in cutting speed leads to a transition from brittleness to toughness, while most of the energy is consumed by plastic flow patterns. Zoei et al. [16] conducted grinding experiments on WC-10Co-4Cr coatings and found that with the increase of cutting depth or feed rate, as well as the decrease of cutting speed, the residual compressive stress value and wear resistance both increased. The increase of residual compressive stress can prevent the formation and propagation of cracks. Kar et al. [17–19] conducted theoretical and experimental research on the grinding of thermal spray coatings and proposed a grinding force model to analyze the fracture behavior of ceramic coatings. The material removal mechanism is mainly due to microbrittle fracture, and the higher the cutting speed, the more obvious the plow marks on the machined surface.

At present, some scholars have studied the damage mechanism of ITO conductive glass. Qiu et al. [20] conducted scratch experiments on ITO glass and found that the mechanical properties of the thin film are affected by internal stress. Increasing the internal compressive stress will improve the hardness of the ITO thin film. Lee et al. [21] compared chemical mechanical polishing with different process parameters to improve the surface quality of ITO films and compared the electrical and optical properties of the polished ITO films. The optimal processing conditions with high removal rate, low non-uniformity, low resistivity, and high transmittance were obtained. Ziaei et al. [22] explained the failure behaviors of layered film systems, such as channel cracking and interfacial delamination, by using a combination of nonlinear finite element method, dislocation-density crystalline plasticity model, and viscoelastic formulation. Wang et al. [23] obtained mechanical performance data such as hardness, elastic modulus, energy release rate, and fracture toughness of ITO thin film materials through nanoindentation tests. They found that plastic deformation and residual stress of the substrate can easily cause local fracture failure of the material.

This article adopts the method of microscale grinding to process ITO conductive glass, in order to explore the material removal mechanism of ITO conductive glass and analyze the influence of process parameters on the surface quality of the processed surface. The grinding force, surface roughness, sheet resistance, and machining morphology in microgrinding experiments were analyzed and studied in the experiment. And soda-lime glass without ITO film was set as the control group of the experimental material, and the effect of the film on the substrate glass material during microgrinding was analyzed.

2 Microscale grinding mechanism of ITO conductive glass

Brittle fracture removal, ductile brittle removal, and ductile removal are the main removal methods for brittle materials. Brittle fracture removal is caused by the formation, propagation, peeling, and fragmentation of voids and cracks, which usually cause damage to the surface or subsurface of the material. The removal of ductile brittleness involves the deformation and peeling of materials, which gradually accumulate with the action of abrasive particles until the material detaches. Ductile removal is the formation of plastic chips under the plowing action of abrasive grains, and the fracture of chips does not cause cracks to spread to the subsurface of the processed workpiece [24–26].

The material removal method during the grinding process can be analyzed by the critical cutting depth h_c and the undeformed chip thickness h_m [27–30]. The undeformed chip thickness for vertical surface grinding can be obtained from the following equation [7]:

$$h_m = \frac{f}{nC_1\left[1+\left(\frac{B}{2D}\right)^2\right]^{\frac{1}{2}}} \tag{1}$$

where C_1 is linear grain density, B is grinding width, D is tool diameter, f is feed speed, and n is spindle speed.

There are two critical cutting depths h_{c1} and h_{c2} for brittle materials. When the undeformed chip thickness h_m is less than the critical cutting depth h_{c1}, the material is removed in the ductile region through plastic flow and is in the ductile removal mode. When h_m is between h_{c1} and h_{c2}, the material is removed from the ductile to brittle transition zone through plastic flow and crack propagation and is in ductile brittle removal mode. When h_m is greater than h_{c2}, the material is in a brittle fracture removal mode [31], and its formula is as follows:

$$h_m = \begin{cases} h_m \le h_{c1} & \text{ductile} \\ h_{c1} < h_m < h_{c2} & \text{brittle} - \text{ductile} \\ h_{c2} < h_m & \text{brittle} \end{cases} \tag{2}$$

On the basis of Bifano's critical cutting depth theory [32], Ma et al. [33] obtained that the critical cutting depth for brittle ductile transition can be calculated by the following equation:

$$h_c = \frac{2K_d \sin^3\theta \cos\theta}{\pi}\left(\frac{K_{IC}}{H}\right)^2\sqrt{\frac{E}{H}} \tag{3}$$

$$h_1 = n_1 h_c \tag{4}$$

$$h_2 = n_2 h_c \tag{5}$$

where θ is the half-angle of grain conic node, K_d is dynamic coefficient, K_{IC} is fracture toughness, E is elasticity modulus, H is microhardness, and η_1 and η_2 are coefficients of ductile stage.

The surface of ITO conductive glass has a brittle thin film, and the fracture toughness of soda-lime glass adjacent to this film area is affected by the bonding effect of the film. However, due to the fact that the thickness of ITO thin films is much smaller than the thickness that can be achieved by microgrinding, the impact on the critical cutting thickness of soda-lime glass is relatively small. When using thin film materials, two factors need to be further corrected. η_1 and η_2 are two ductility stage coefficients.

The microgrinding mechanism of ITO conductive glass is shown in Fig. 2, where Fig. 2a is a schematic diagram of microscale grinding. Microgrinding tool with electroplated abrasive particles with a diameter of less than 1 mm is used to machine microgrooves on ITO conductive glass. The material of the workpiece is ITO conductive glass, which is based on soda-lime glass and coated with an ITO thin film with a thickness of 0.2 μm on the surface.

Figure 2b shows the material removal mechanism of ITO conductive glass under microscale abrasive action. At this time, the cutting thickness h is less than the critical cutting depth of the glass, and the glass substrate is in a ductile removal state. However, due to the large elastic modulus and thin thickness of the ITO film, it is in a brittle fracture removal state. In Fig. 2b, under the influence of the radius effect of the abrasive cutting edge, a shear deformation zone appears at the front end of the abrasive. The plow with abrasive grains exerts a squeezing force F_1 on the surface of the material, leaving ductile scratches on the processed surface. When ductile chips are formed, F_2 in the shear deformation zone tears and separates the chips from the workpiece. The material strength resists the extrusion force F_3 generated by deformation. The higher material strength of the

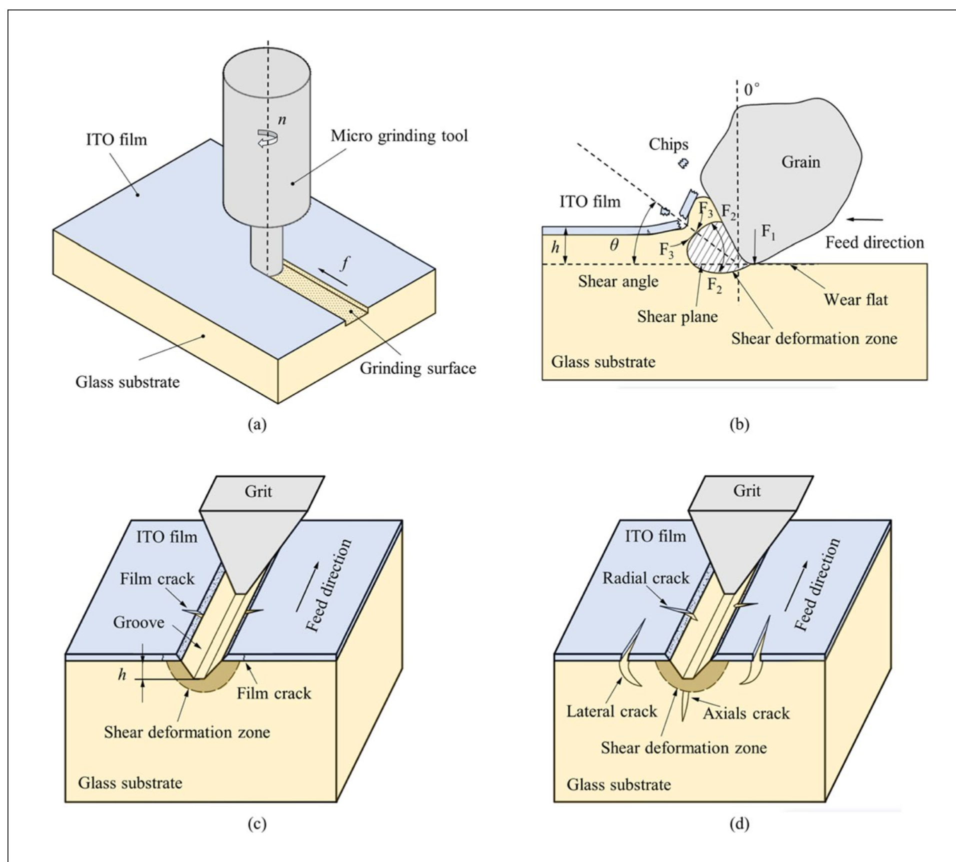

Fig. 2 Microgrinding mechanism of ITO conductive glass. **a** Microgrinding schematic diagram. **b** Material removal mechanism. **c** Ductile removal of substrate. **d** Brittle removal of substrate

thin film layer itself enhances F_3 to a certain extent, hinders the shear deformation of the substrate, reduces the shear angle θ, increases the shear plane, and compresses the shear deformation zone.

Figure 2c shows the removal mechanism of ITO conductive glass under the ductile removal mode of glass substrate. When the cutting depth is shallow, the glass material in the shear deformation zone is separated from the material surface mainly by plastic flow [34, 35]. Due to the small thickness of the film, there is not enough area to produce plastic flow. Under the action of abrasive particles, cracks and burrs are generated at the scratch edge of ITO film. The bonding force between layers fails to inhibit the crack propagation of ITO film, and ITO film is still in the state of brittle removal. At the same time, the shear deformation of the glass substrate will also cause more cracks in the film.

Figure 2d shows the brittle removal mechanism of ITO conductive glass. When abrasive particles scratch the workpiece, axial cracks and lateral cracks are generated at the bottom and edges of the shear deformation zone on the glass substrate. Radial cracks are also generated at the edge of the scratch. At the same time, cracks are also generated in the thin film layer under stress, and these cracks extend to produce brittle chips [36]. In addition, thin film failure forms such as delamination and fracture may occur during the processing. Among them, delamination refers to the failure of the bonding between the film and the substrate, resulting in the film falling off. Interlayer fracture refers to the extension of interlayer cracks to the point of penetration, resulting in the complete peeling of the material [37, 38].

3 Experimental methods and equipment

As shown in Fig. 3, a microgrinding experiment was conducted on a CNC machining center (VMC5640V4). The workpiece was installed on a force measuring instrument (MC3D160) and fixed on the machine tool workbench through a vacuum chuck. The measured data was input to the PC port for real-time analysis and processing through a signal acquisition card (MCD3USB). The surface profile and roughness were measured using a superdepth microscope (DSX1000), the resistance of the processed thin film was measured using a four probe square resistance meter (HP2523), and the microstructure of the processed surface was analyzed using a scanning electron microscope (SEM3100).

As shown in Fig. 4a, the size of the ITO conductive glass workpiece is $25 \times 50 \times 2$ mm, with an ITO film thickness of 0.2 μm. The sheet resistance of the thin film is 6.8Ω. Select the 500# electroplated diamond grinding tool

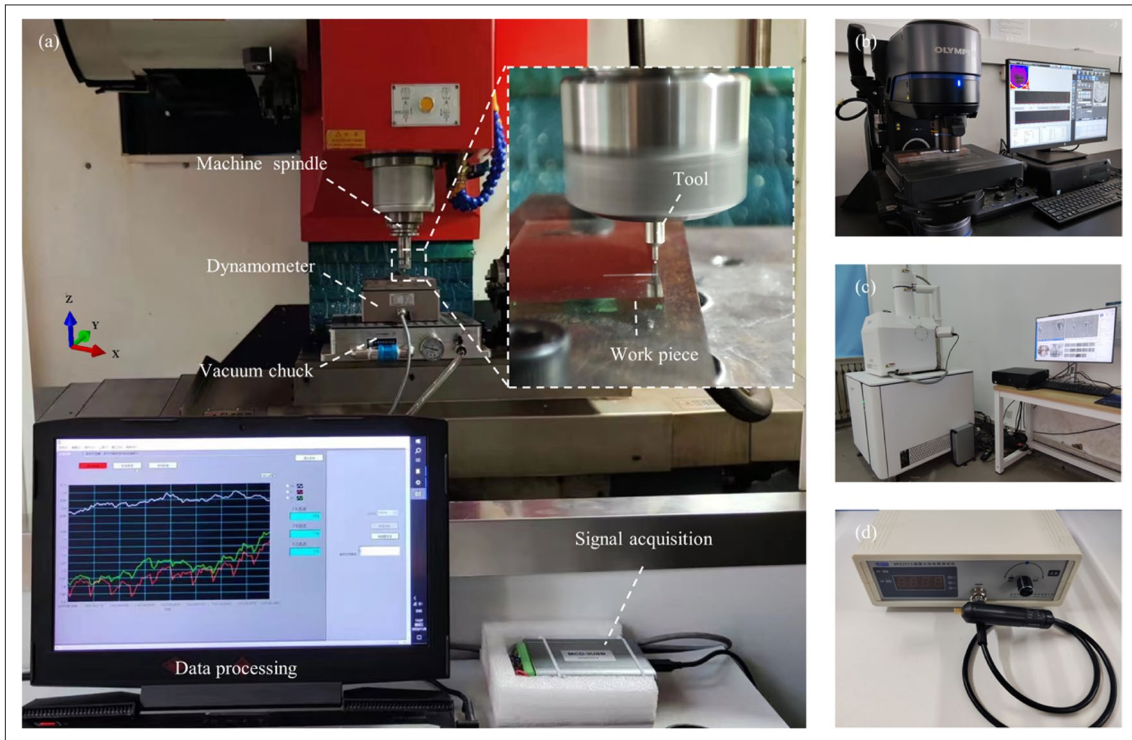

Fig. 3 Experimental platform and equipment. **a** Experimental platform. **b** DSX1000 superdepth microscope. **c** SEM3100 scanning electron microscope. **d** HP2523 four probe square resistance meter

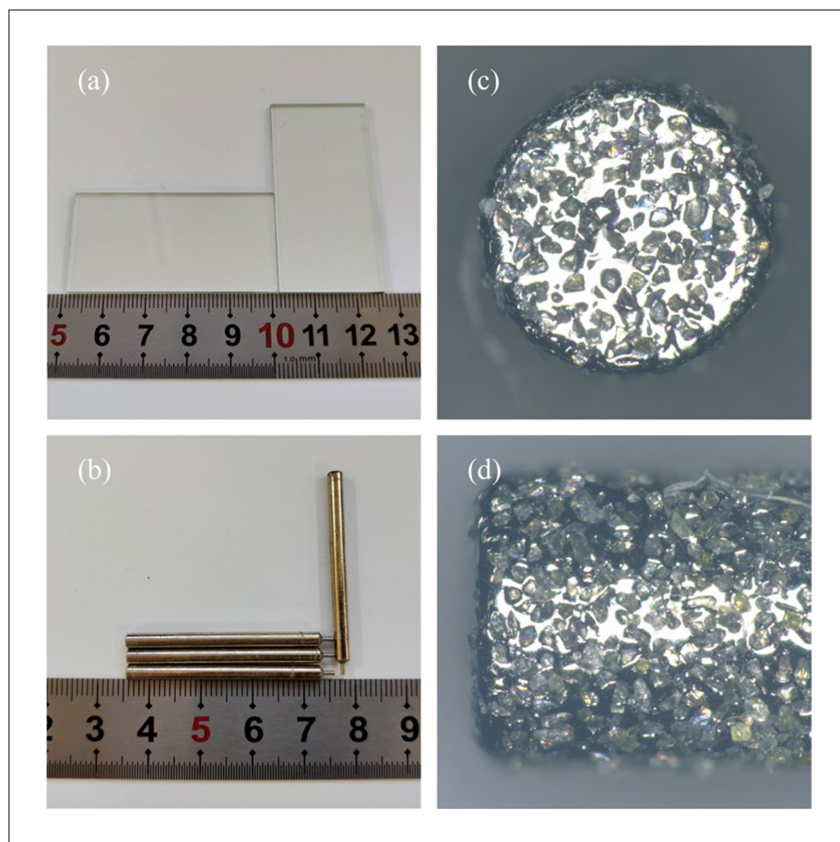

Fig. 4 Workpiece and tool. **a** ITO conductive glass. **b** Electroplated microgrinding tool. **c** End face morphology of microgrinding tool. **d** Lateral morphology of microgrinding tool

Table 1 Material properties

Material	Density ρ (kg/m^3)	Elastic modulus E (GPa)	Poisson's ratio	Tensile strength σ_t (MPa)
ITO film	6800	116	0.35	293
Soda-lime glass	2530	62	0.23	53
Diamond	3520	1100	0.17	–

as shown in Fig. 4b for the experiment, and the tool morphology is shown in Fig. 4c, d. At the same time, soda-lime glass is set as the experimental control group to analyze the material removal mechanism of ITO conductive glass. The specific properties of the workpiece and tool materials are shown in Table 1.

In order to study the influence of process parameters on the processing quality of ITO conductive glass, processing tests are carried out on the material within the range of these parameters as shown in Table 2. After finishing the microgrinding of each parameter, the grinding tool is dressed to keep the same state. In addition, new grinding tools are replaced after each group of tests to ensure the accuracy of the tests.

The logic structure of the overall test is shown in Fig. 5. The single factor test of ITO conductive glass was carried out. With $n = 7000$ r/min, $f = 1$ mm/min, a_p=9 μm is the standard, changing one of the factors. The variations of grinding force, surface roughness, and sheet resistance were measured under the condition of changing this factor. To analyze the influence of processing parameters on processing quality and material properties, soda-lime glass without ITO film was set as the control group for comparative test. The influence of thin film on microgrinding process is analyzed through the difference of microgrinding force and surface roughness. In addition, the orthogonal test of three factors and four levels is carried out on ITO conductive glass within the parameter range shown in Table 2. The influence of processing parameters on processing quality is analyzed by taking surface roughness and film resistance as evaluation indexes. Determine the main factors affecting the processing quality and the optimal parameter combination.

4 Discussion of experimental results

4.1 Analysis of microgrinding force

Grinding force is the force applied to the tool or workpiece during the grinding process, which can to some extent reflect the processing state of the material [30]. Studying the microgrinding force of ITO conductive glass can determine the influence of microgrinding process parameters on machining efficiency and analyze the removal state of materials. By comparing with soda-lime glass, the material removal mechanism of ITO conductive glass can be further studied.

Table 2 Microgrinding experimental design

Factors	Range
Spindle speed n (r/min)	5000~8000
Feed speed f (mm/min)	0.5~2
Cutting depth a_p (μm)	3~21

Figure 6 shows the fluctuation curve of tangential force with microgrinding time obtained by grinding ITO conductive glass and soda-lime glass using a 500# electroplated diamond microgrinding tool. It can be seen that under the same microgrinding parameters, the tangential force experienced by the two materials during microgrinding fluctuates within a certain range, but the tangential force of ITO conductive glass is larger than that of soda-lime glass. The highlighted blue area in Fig. 6 represents the effect of the presence of ITO film on grinding force. This indicates that the material strength of ITO film is greater than that of soda-lime glass. Even though the thickness of ITO film layer accounts for a small proportion of the microgrinding thickness, this effect can still be reflected in the microgrinding force, which affects the processing performance of ITO-coated glass.

Figure 7 shows the graph of the tangential force of ITO conductive glass and soda-lime glass microgrinding as a function of process parameters. In Fig. 7a, it can be seen that the tangential force of the two materials increases with the increase of cutting depth. This is because the deeper the cutting depth, the larger the volume of the grinding tool, and at the same time, the area of contact between the abrasive particles and the workpiece increases, resulting in an increase in the frictional force generated by microgrinding. In addition, the tangential force of soda-lime glass in Fig. 7a is always smaller than that of ITO conductive glass. This is because ITO conductive glass has an additional layer of ITO film compared to soda-lime glass, and the presence of the film increases the surface hardness of the glass substrate. When cutting with microgrinding tools, the abrasive particles need to consume more energy to overcome the ITO film, so microgrinding of ITO conductive glass will generate greater tangential force. When the cutting depth is low, the size effect of microscale grinding makes the tangential force difference more pronounced. In order to clearly show the influence of ITO film on grinding force, the film effect e_f is defined as

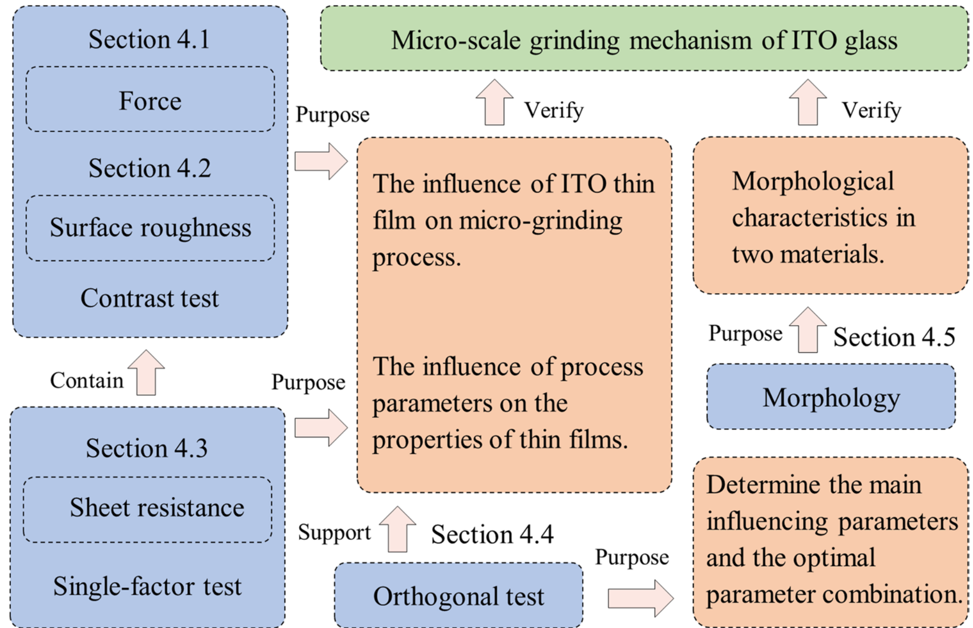

Fig. 5 Logical structure of experiment

$$e_f = \frac{F_i - F_s}{F_i} \times 100\% \tag{6}$$

where F_i is the grinding force of ITO conductive glass and F_s is the grinding force of soda-lime glass.

According to the film effect curve in Fig. 7a, it can be found that with the increase of cutting depth, the contribution of film to grinding force gradually decreases by about 10%. This is because the thickness of ITO film is fixed, and the effect of the film on the tangential force is masked by the increasing cutting depth.

Figure 7b shows that as the feed rate increases, the tangential forces of the two materials also increase accordingly. An increase in feed speed will result in a greater amount of material removal per unit time, requiring greater tangential force to maintain the given feed speed. According to the film effect curve, it can be seen that ITO film will affect the tangential force in the grinding process.

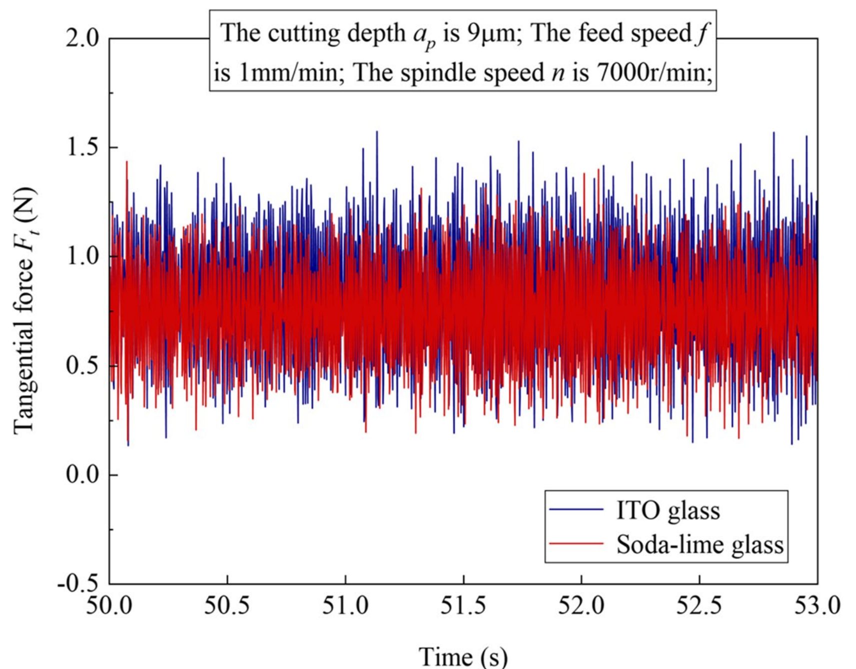

Fig. 6 Tangential force fluctuation curve of two materials

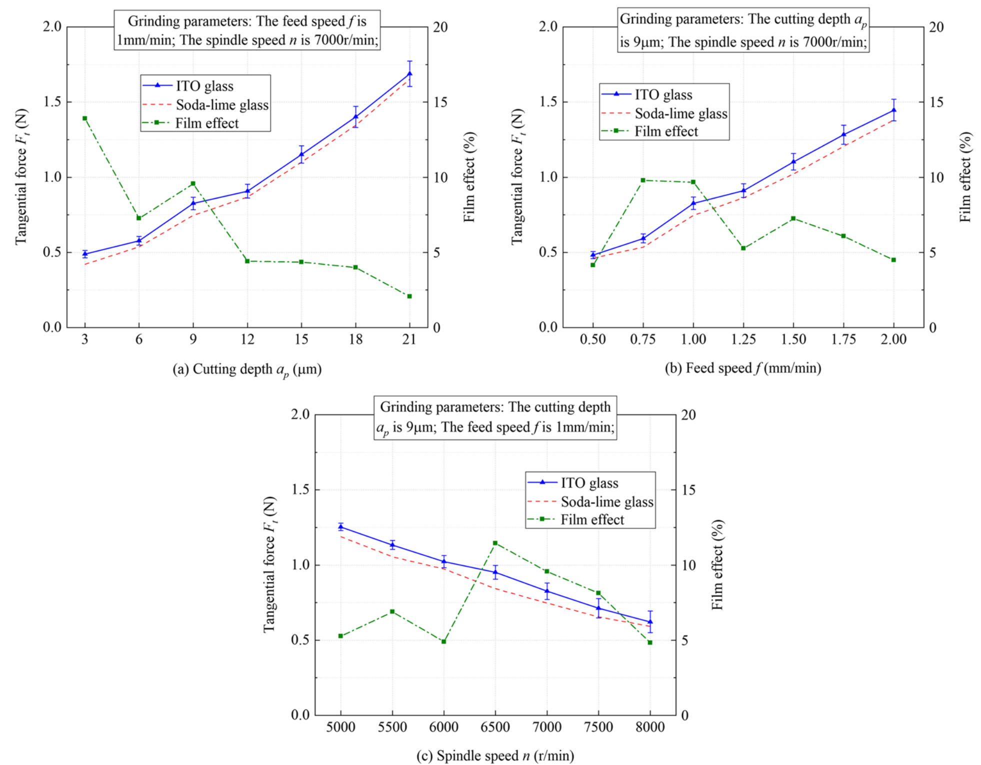

Fig. 7 Tangential force of two materials with different parameters. **a** Tangential force at different cutting depths. **b** Tangential force at different feed speeds. **c** Tangential force at different spindle speeds

The influence of film on the cutting force fluctuates at 7% of the total tangential force, and the change with the feed speed is not obvious.

In Fig. 7c, it can be observed that the tangential force increases with the increase of spindle speed. The reason is that increasing the spindle speed will improve the abrasive effect on the microgrinding tool, and more abrasive particles will participate in cutting per unit time, thereby reducing the volume of single abrasive particle removal and reducing grinding force. In addition, increasing the spindle speed will steadily increase the grinding area, thereby improving microgrinding performance and reducing grinding force. The increase of spindle speed will gradually reduce the difference of tangential force between ITO conductive glass and soda lime glass. The reason is that increasing the spindle speed will result in more abrasive particles being cut per unit time, and the effect of ITO film on material removal is weakened by the spindle speed.

4.2 Analysis of surface roughness

Surface roughness is an important indicator for evaluating the quality of processed surfaces. The variation curve of surface roughness with process parameters during microscale grinding of ITO conductive glass and soda-lime glass is shown in Fig. 8. It can be observed that the greater the cutting depth, the greater the surface roughness of the machined surface in Fig. 8a. This is because as the cutting depth increases, the volume of removed glass substrate increases, resulting in an increase in powdered chips that accumulate in the gaps between abrasive particles, hindering the flow of chips and reducing the effective cutting area of abrasive particles. When the microgrinding tool is fed, the chips accumulated between the gaps of the abrasive particles will cause obvious cutting marks and pits to appear on the machining surface. At the same time, an increase in cutting depth will lead to an increase in cutting force. Excessive stress will cause brittle glass materials to reach their strength limit, resulting in shear deformation, fragmentation, or peeling.

Comparing the two curves in Fig. 8a, it can be observed that the surface roughness of ITO conductive glass is greater than that of soda-lime glass. The reason is that ITO films have higher material strength compared to glass substrates. Under the action of microscale grinding, stress concentration causes the glass substrate to reach the damage criterion before the ITO film. When the stress reaches the damage strength of the ITO film, under the action of the adhesion force between the film and the substrate, the glass substrate further undergoes greater damage.

Comparing the two curves in Fig. 8a, it can be observed that the surface roughness of ITO conductive glass is greater than soda-lime glass. The reason is that ITO films have higher material strength compared to glass substrates. Under the action of microscale grinding, the glass substrate reaches the damage criterion before the ITO film. When the

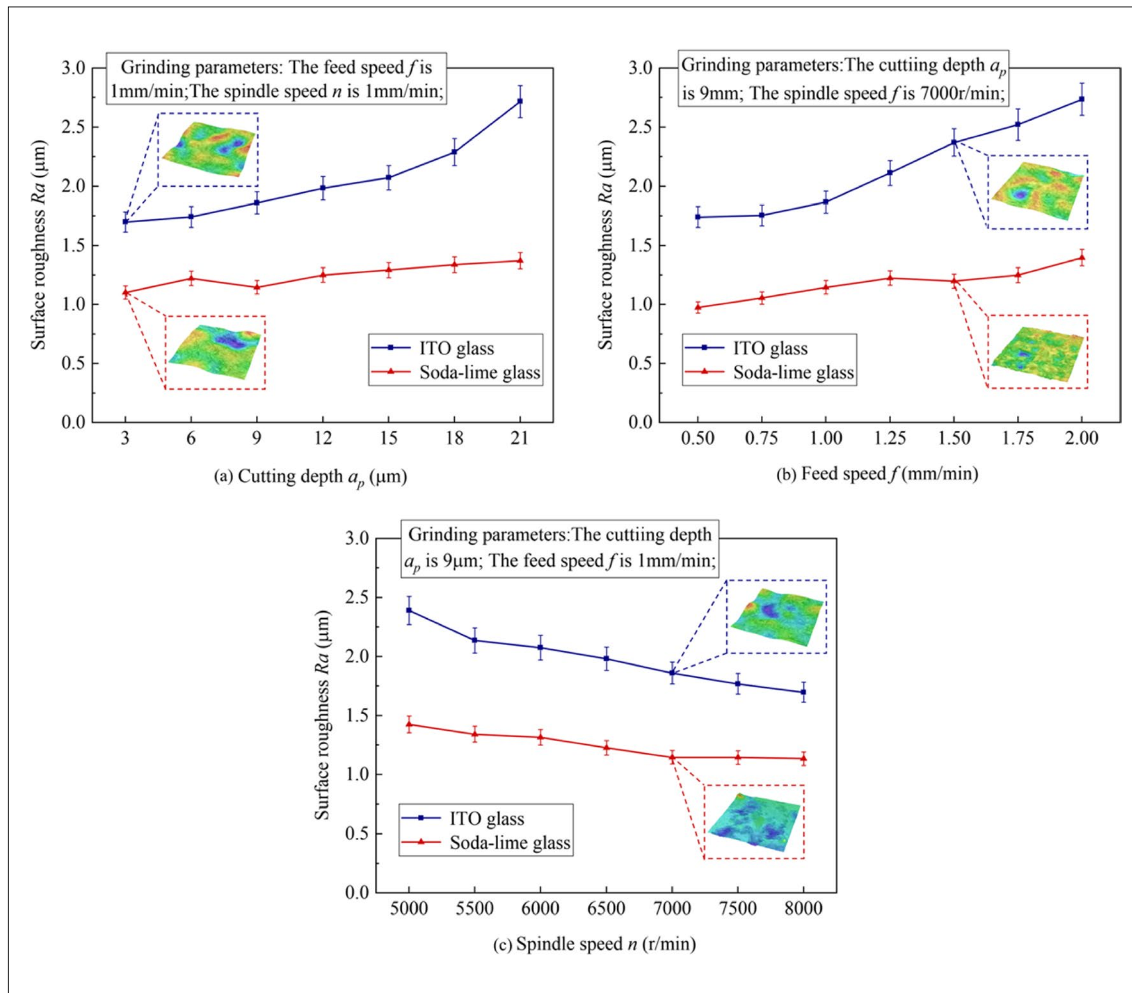

Fig. 8 Surface roughness variation curves of two materials. **a** Surface roughness variation curve with cutting depth. **b** Surface roughness curve with feed speed. **c** Surface roughness variation curve with spindle speed

stress reaches the damage strength of the ITO film, under the inhibitory effect of the film on substrate shear deformation, the glass substrate further undergoes greater damage. The presence of ITO thin film layers makes it more difficult to obtain high-quality machined surfaces.

Figure 8b shows that the machined surface roughness increases with the increase of feed speed. Due to the fact that glass is an amorphous brittle material, an increase in feed speed during microgrinding can lead to a transition from ductile brittle removal to brittle removal, resulting in brittle fracture and an increase in surface roughness. It can be found that the surface roughness of ITO conductive glass processing is significantly higher than that of soda-lime glass due to the influence of feed speed. Under the influence of higher feed speed and interlayer cohesion of the film, interlayer cracking between the film and substrate can cause cracks and defects in the glass substrate, leading to a decrease in the quality of microgrinding processing.

Figure 8c shows the variation curve of machining surface roughness with microgrinding spindle speed. As the spindle speed increases, the surface roughness decreases accordingly. According to the brittle fracture criterion, cracks propagate along the path with the highest energy release rate [39, 40]. As glass is a brittle material, the energy is small at low spindle speeds, and the material is mainly removed through brittle fracture. As the spindle speed increases, the material removal method gradually switches to ductile removal. In addition, increasing the spindle speed will increase the cutting efficiency of the abrasive particles on the microgrinding tool, allowing the chips to flow quickly and detach from the microgrinding tool, eliminating protrusions and burrs that affect the machining surface roughness, and thereby reducing the surface roughness [41]. Comparing the variation curves of the two materials, it can be observed that the numerical difference in surface roughness gradually narrows with the increase of spindle speed. This indicates that higher

spindle speeds are easier to process ITO films, and increasing spindle speed helps to break the bonding state between ITO films and glass substrates.

The surface roughness *Ra* obtained by microgrinding ITO conductive glass is in the range of 1.5 to 3.0 μm, while *Ra* of soda-lime glass is in the range of 1.0 to 1.5 μm. The surface roughness of soda-lime glass is only about 60% of ITO conductive glass. The existence of ITO film layer makes it more difficult to obtain high-quality machined surface.

4.3 Analysis of sheet resistance

In order to investigate the influence of microscale grinding on the conductivity of ITO thin films, a four probe square resistance meter was used to measure the sheet resistance of the thin film at the edge of the microgroove on ITO conductive glass. At the same time, the edge crack amount of the microgroove captured by a superdepth microscope was calibrated, as shown in Fig. 9.

By organizing experimental data, Fig. 10 shows the influence of microscale grinding process parameters on the conductivity and edge crack of ITO conductive glass. The bar graph represents the amount of edge crack, and the line graph represents the sheet resistance of the thin film. The edge crack caused by microscale grinding directly affects the integrity of the thin film at the edge of the microgroove, and the microcracks generated by the edge collapse can change the structure of the ITO thin film, causing the conduction of current at the crack to be hindered. Therefore, there is a correlation between the sheet resistance of the thin film and the amount of edge crack. But this relationship is not absolute, and the integrity of the film is also affected by factors such as chip splashing, high-temperature burns, and subsurface damage during microgrinding.

In the microgrinding test of ITO conductive glass, the edge crack of the microgroove fluctuated in the range of 10 to 45 μm, and the measured sheet resistance ranged from 16.0 to 18.0 Ω. The fluctuation of edge crack amount and sheet resistance with the change of processing parameters is similar, and the two indicators reflect the integrity of the edge surface of the microgroove. As shown in Fig. 10, the influence of microgrinding process parameters on film quality can be analyzed by making it into a double Y-axis graph.

Figure 10a shows the effect of cutting depth on conductivity and edge crack. The sheet resistance and edge crack show an overall upward trend with increasing cutting depth. However, when the cutting depth is shallow, the microgrinding tool does not have sufficient contact with the material, resulting in local stress concentration and easy edge crack at the edge of the microgroove. In addition, the smaller cutting depth highlights the brittle and hard material characteristics of ITO films, which can cause delamination between ITO films and substrates during microscale grinding, affecting the conductivity of the films.

Figure 10b shows the effect of feed speed on the amount of edge crack and the sheet resistance of the thin film. At low feed speed, grinding is relatively stable, and the variation amplitude of edge crack and sheet resistance is relatively small. When the feed speed increases to a certain range, it will lead to an increase in the cutting thickness of the abrasive particles, resulting in an increase in grinding force. The pressure between the tool and the workpiece increases

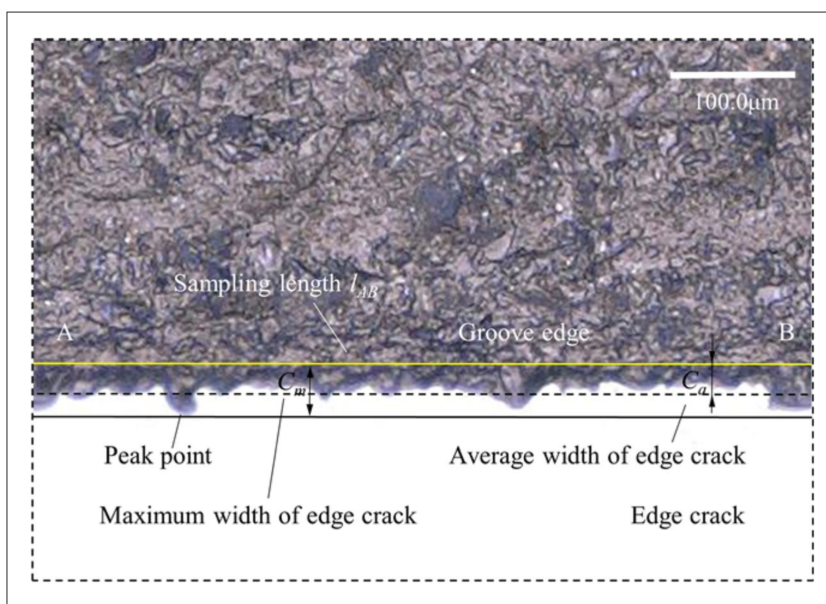

Fig. 9 Measurement of edge crack

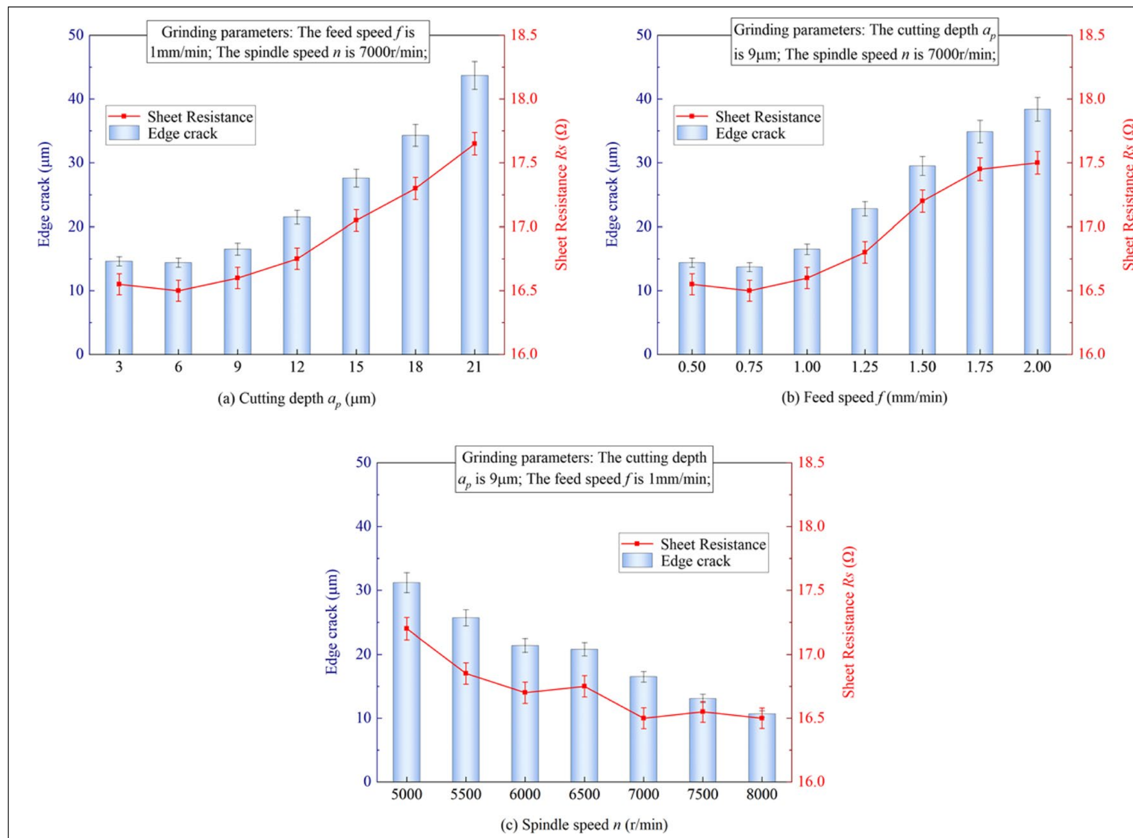

Fig. 10 Edge crack and sheet resistance under different parameters. **a** Edge crack and sheet resistance at different cutting depths. **b** Edge crack and sheet resistance at different feed speeds. **c** Edge crack and sheet resistance at different spindle speeds

beyond the material strength limit, and the brittle fracture of the material affects the values of the sheet resistance and edge crack. Due to the subsurface damage generated during microscale grinding, defects appear at the bonding interface between ITO film and glass substrate, resulting in a mismatch between the sheet resistance and the amount of edge crack under certain parameters.

Figure 10c shows the effect of spindle speed on the amount of edge crack and sheet resistance. The amount of edge crack decreases with the increase of microscale grinding spindle speed. The reason for this is that the higher the spindle speed, the better the chip flow state during microgrinding and the more abrasive particles come into full contact with the material. In addition, increasing the spindle speed will reduce the material removal volume of abrasive particles, reduce cutting force, and thus improve the machining status of microgrinding tools. However, due to the increase in spindle speed, the kinetic energy of chips will be increased, and chips flying away from the substrate will collide with micropits at the edge of the microgrooves. These microdamages will affect the integrity of the ITO film, thereby affecting the sheet resistance.

4.4 Analysis of orthogonal experiments

Surface roughness and sheet resistance are important evaluation indexes of microgrinding quality and material properties of ITO conductive glass. In order to determine the importance of each factor on the processing quality and find the optimal parameter combination, this paper designs an orthogonal test with three factors and four levels. The specific data obtained from the orthogonal test are shown in Table 3.

Perform range and variance analysis on the data in Table 3, and the results are shown in Fig. 11. Among them, Fig. 11a, b, respectively, represents the variation of surface roughness and sheet resistance k values with orthogonal levels under various factors. Surface roughness reflects the quality of the processed surface, while sheet resistance reflects the influence of processing on the conductivity of the material. These two indicators have slightly different trends with changes in processing parameters. Performing range analysis can obtain Fig. 11c, where the maximum influencing factor on surface roughness is spindle speed, while the maximum influencing factor on sheet resistance is cutting

Table 3 Orthogonal test table for microgrinding ITO conductive glass

No.	n (r/min)	f (mm/min)	a_p (μm)	Ra (μm)	Rs (Ω)
1	5000	0.5	3	1.937	17.15
2	5000	1	9	2.356	17.30
3	5000	1.5	15	2.592	17.55
4	5000	2	21	2.805	18.00
5	6000	0.5	9	1.941	17.40
6	6000	1	15	2.153	17.60
7	6000	1.5	21	2.618	17.80
8	6000	2	3	2.456	17.40
9	7000	0.5	15	2.152	17.30
10	7000	1	21	2.725	17.50
11	7000	1.5	3	2.065	17.25
12	7000	2	9	2.648	17.65
13	8000	0.5	21	1.979	17.15
14	8000	1	3	1.632	16.85
15	8000	1.5	9	1.816	17.15
16	8000	2	15	1.927	17.55

depth. The analysis of variance in Fig. 11d can further analyze the dispersion degree in the data distribution.

In the analysis of variance, the dispersion degree of surface roughness is large under the spindle speed, which means that the surface roughness is significantly affected by the spindle speed. This is because high spindle speed will make the abrasive particles contact with the material more fully, and the machined surface will be more uniform. At the same time, increasing the spindle speed can reduce the amount of edge crack the microgroove, but this will make the chip obtain more kinetic energy, causing many small pits in the ITO film layer at the edge of the microgroove. These tiny defects will affect the film structure and weaken the conductivity of the film. Increasing the spindle speed has little effect on reducing the sheet resistance at the edge of the microgroove. Therefore, in the variance analysis in Fig. 11d, the dispersion degree of the film square resistance is small under the spindle speed.

The cutting depth has the most significant effect on the sheet resistance. This is because the larger the cutting depth, the larger the volume of material removed in the microgrinding process. This means that more chips and edge cracks will cause more damage to the edge of the microgroove and increase the sheet resistance. In addition, the chips between the abrasive spaces are difficult to flow and accumulate due to the cutting depth, which reduces the quality of microgrinding [42], and the resulting cracks and subsurface damage will also damage the microstructure of the film and affect the conductivity of the material. Through orthogonal analysis, the optimal process parameters of ITO conductive glass microgrinding quality are obtained as follows: $n=8000$ r/min, $f=0.5$ mm/min, a_p=3 μm.

The microgroove morphology corresponding to each group of parameters in the orthogonal test was photographed by using the superdepth microscope, as shown in Fig. 12. It can be seen that the surface quality of no. 14 microgroove is the highest, and the ductile removal mode dominates the material removal process of microgrinding. The formation process of microgroove machined surface involves complex abrasive mechanism. As shown in Fig. 13, microgrinding area can be divided into main grinding area, plow area, and sliding area [43].

Most of the chips in the microgrinding process are formed in the main grinding area. After the external abrasive

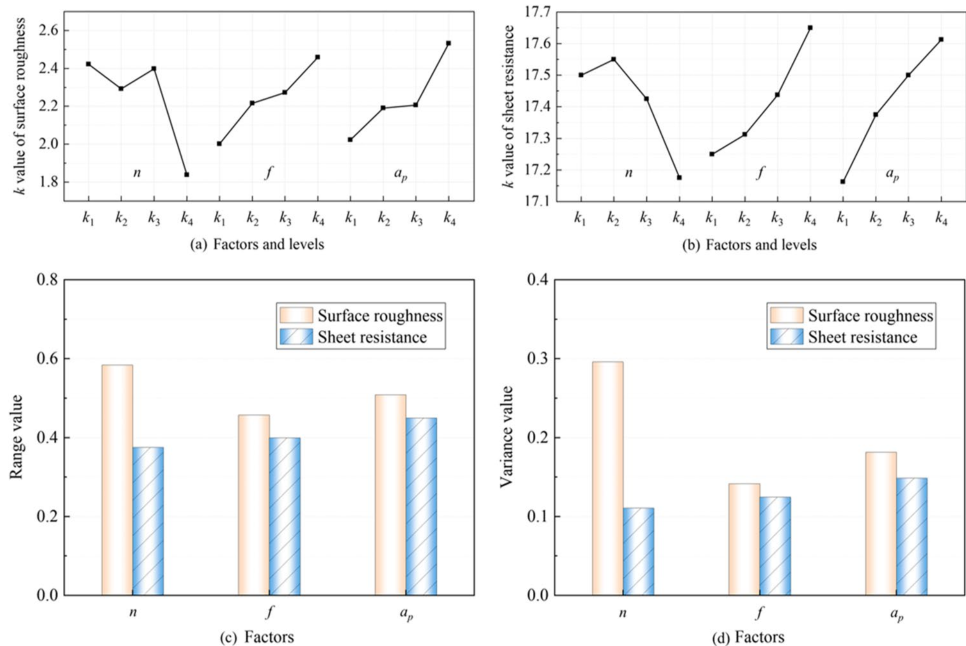

Fig. 11 Analysis of orthogonal test results. **a** k value analysis of surface roughness. **b** k value analysis of sheet resistance. **c** Range analysis of two indicators. **d** Variance analysis of two indicators

Fig. 12 Microgroove morphology of ITO conductive glass under different microgrinding parameters

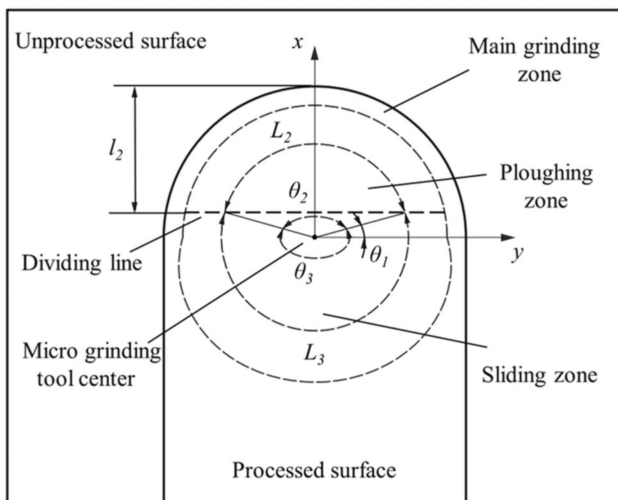

Fig. 13 Microgrinding area division

particles on the end face of the microgrinding tool pass through, the internal abrasive particles further plough the workpiece. As shown in Fig. 12, the increase of feed speed will lead to the increase of the area of the main grinding area. When the external abrasive grains of the microgrinding tool are damaged, the internal abrasive grains will also be involved in the formation of chips. At this time, the grinding marks of the internal abrasive grains will be left on the machined surface. As shown in Fig. 12, higher spindle speed will damage the external abrasive particles and easily leave grinding marks on the machined surface.

In the sliding friction area, the abrasive particles generate pressure and friction with the workpiece, and the workpiece material only has elastic deformation. However, when the cutting depth increases, the chip removal of the microabrasive tool is difficult, which causes greater friction in the sliding area and reduces the processing quality. The boundary between plow area and sliding area changes with the change

of grinding parameters. A chord on the circumference of the microabrasive tool is defined as the boundary between the two areas, and the abrasive particles are at the angle of rotation θ_2 internal plough, at the corner θ_3 internal sliding friction. Increasing the spindle speed will reduce θ_2 corners, compressing the plow area.

4.5 Analysis of microgrinding morphology

As shown in Fig. 14a, the microgrinding morphology comparison of ITO conductive glass and soda-lime glass under the same process parameters is shown. Under the illumination of a specific superdepth microscope, the ITO film under the microscope lens appears green, while soda-lime glass without the film does not have this feature. Compared to soda-lime glass, the processed surface color of ITO conductive glass is darker and more turbid. This is because the high-strength ITO film suppresses the shear deformation of the substrate glass, resulting in greater cutting force. The friction between microgrinding tools and materials generates high temperatures, causing burns on the glass substrate [44]. The peeling and fracture of ITO film during microgrinding process result in more damage such as micropits, micromarks, and microcracks on the machined surface.

As shown in Fig. 14b, after microgrinding, ITO conductive glass will have small pits at the edge of the microgrooves, which is the damage caused by the splashing chips during the microgrinding process to the surface of the thin film. These damages can damage the microstructure of the film surface, thereby affecting the conductivity of the material. At the same time, the size and shape of micropits are influenced by microscale grinding process parameters, so the film resistance can to some extent reflect the integrity of ITO films.

Comparing the edge crack of the two material microgrooves in Fig. 14a, it can be observed that the edges of ITO glass are continuous large pieces of edge collapse, while the edges of soda-lime glass microgrooves are intermittent small pieces of edge collapse. This is because the ITO film has a higher hardness, and its presence suppresses crack propagation on its glass substrate. Under the action of microgrinding, the glass substrate of ITO conductive glass undergoes subsurface damage, leading to stress concentration in the ITO film layer. Cracks at the edge of the film extend and

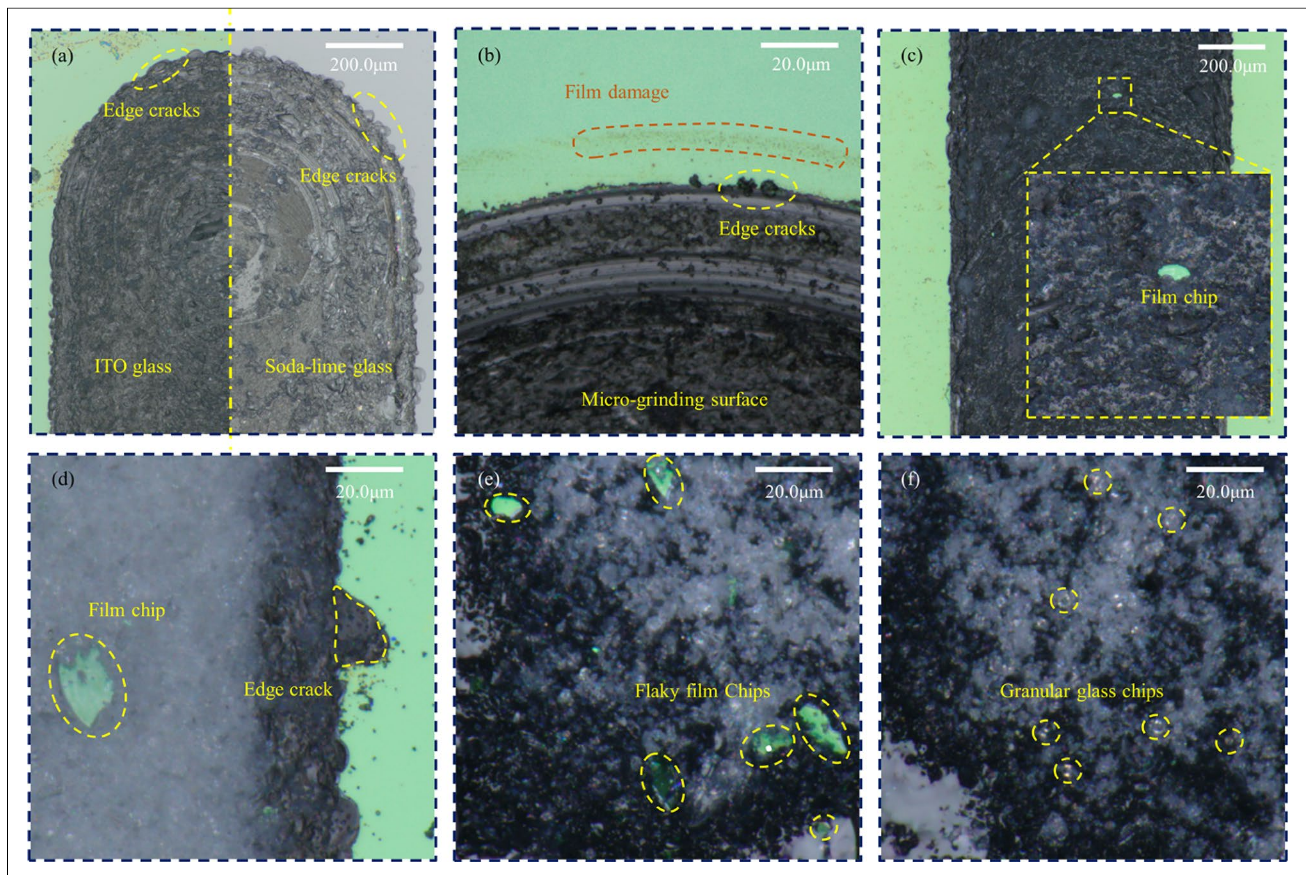

Fig. 14 Microgrinding morphology. **a** Microgroove morphology of two materials. **b** Film damage. **c** Flaky film chips. **d** Interlayer fracture. **e** Chips of ITO glass. **f** Chips of soda-lime glass

penetrate, forming interlayer fractures. Large pieces of edge crack are caused at the edge of the microgroove, resulting in flaky ITO film chips as shown in Fig. 14c.

Under the action of abrasive particles on microgrinding tools, the ITO film exhibits a brittle fracture removal mode, while the soda-lime glass on the substrate exhibits a ductile brittle removal mode. As shown in Fig. 14d, the chips of ITO film and glass substrate exhibit two different forms, with the flaky chips being ITO film and the powdery chips being glass substrate. This is due to the lower strength of the material compared to the glass substrate, which shatters into smaller particles under the action of microgrinding.

Figure 14e, f shows the chip morphology of microgrinding ITO conductive glass and soda-lime glass. By comparing the two figures, it can be observed that most of the two types of chips are composed of powdered particles, which is consistent with the glass material of ITO conductive glass substrate and soda-lime glass material, resulting in similar chip morphology. There are flaky film fragments in the ITO conductive glass chips, which are due to the fact that the ITO film suppresses the fragmentation of some glass substrates. When the crack in the film layer extends to the through, the interlayer fracture formed will peel off the flaky ITO film and some of its glass substrates, forming flaky chips.

Figure 15 shows the microgrinding morphology of ITO conductive glass captured by SEM, where Fig. 15a shows the microgrinding cutting depth of 9 μm. The microgrooves obtained under the process parameters of feed speed of 1 mm/min and spindle speed of 7000 r/min can show burrs and chips on the edge of the thin film. Due to the stress generated by the ITO film after abrasive sliding, it did not meet the film damage standard. However, the glass on the substrate had already broken prematurely due to its low strength. Subsequently, the edge of the film brittle fractured under the compression of the abrasive, resulting in burrs on the edge of the microgroove.

In Fig. 15b, it can be seen that there is damage generated after microgrinding. Due to the blockage of the abrasive gap

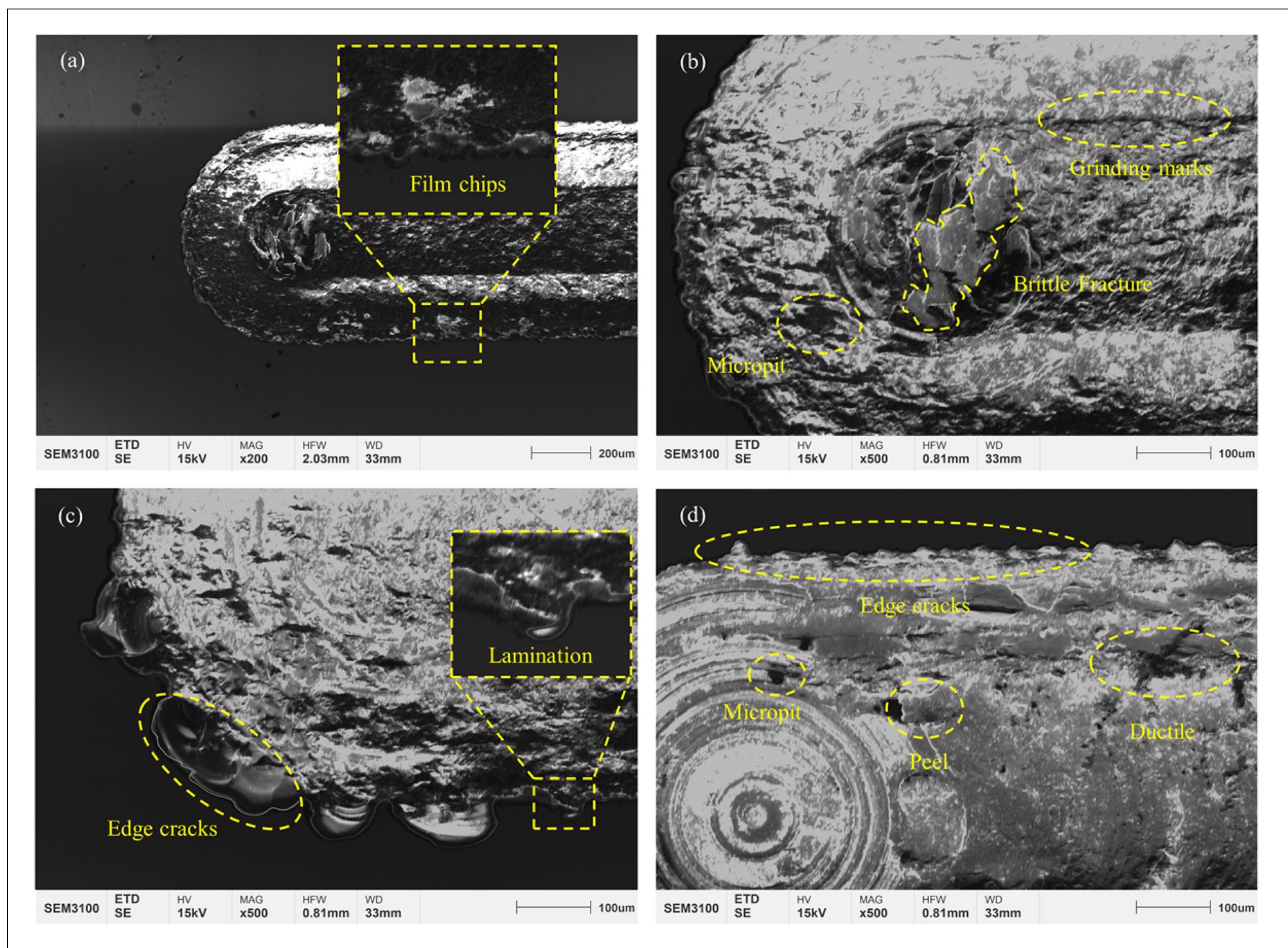

Fig. 15 Microgrooves of ITO glass by SEM. **a** Microgroove morphology. **b** Brittle removal morphology of substrate. **c** Morphology of edge crack. **d** Ductile removal morphology of substrate

by chips during the microgrinding process, some abrasive particles cannot work effectively, leaving defects such as grinding marks and micropits on the machining surface. Meanwhile, some brittle fractures can also be observed, which are caused by the brittle removal mode of the glass substrate.

Figure 15c shows the edge crack of ITO conductive glass during microgrinding, which is caused by process parameters such as low rotational speed, high feed speed, and large cutting depth. There is a strong adhesion between the thin film layer of ITO conductive glass and the substrate. When the glass edge is broken, the ITO thin film will peel off together with the glass substrate. The presence of the thin film layer and the phenomenon of delamination with the glass substrate can be found at the edge of the broken edge.

Figure 15d shows a different microgrinding morphology from the previous figures. When the microgrinding spindle speed is 8000 r/min, the feed speed is 1 mm/min, and the cutting depth is 9 µm, the surface of the microgrinding will exhibit ductile deformation and peeling, and the edge crack will appear as a serrated morphology, showing an overall ductile removal state. At this point, the ITO film at the edge of the microgroove exhibits small brittle fracture morphology features, while the glass substrate at the bottom of the microgroove exhibits ductile removal morphology features.

5 Conclusion

1. The film on the surface of ITO conductive glass will inhibit the shear deformation of the substrate material, thus affecting the material removal state of the material in microgrinding.
2. Compared with soda-lime glass, ITO conductive glass has higher grinding force and lower processing quality during microgrinding. The existence of ITO film makes high-quality grinding of materials more difficult.
3. In the microgrinding of ITO conductive glass, increasing the rotating speed, reducing the feed rate, and reducing the cutting depth will improve the quality of the microgroove. Among them, the surface roughness is significantly affected by the spindle speed, and the sheet resistance is significantly affected by the cutting depth.
4. The chips of ITO film are mainly flake film chips produced by brittle fracture. The chips on the glass substrate are mainly powder chips.
5. The thin film layer of ITO conductive glass shows brittle fracture removal characteristics in microgrinding. But the substrate shows ductile or brittle removal characteristics with different processing parameters.

Author contribution All authors contributed to the study conception and design. Material preparation, data collection, and analysis were performed by Xiaolong Qiu, Yin Liu, and Fei Pan. The first draft of the manuscript was written by Xiaolong Qiu and Yin Liu. Experimental tests were carried out by Xiaolong Qiu. All authors read and approved the final manuscript.

Funding This research was supported by National Natural Science Foundation of China (Grant Nos. 52005346 and U1908230), Natural Science Foundation of Liaoning Province (Grant No. 2021-BS-149), Project of Liaoning Province Applied Basic Research Program (Grant No. 2022JH2/101300214), and Scientific Research Funding Project of Liaoning Provincial Department of Education (Grant No. LQGD2020017), .

Declarations

Ethics approval Not applicable.

Consent for publication The authors consent to publish this article.

Consent to participate Not applicable.

Competing interests The authors declare no competing interests.

References

1. Thirumoorthi M, Prakash JTJ (2016) Structure, optical and electrical properties of indium tin oxide ultra thin films prepared by jet nebulizer spray pyrolysis technique. J Asian Ceam Soc 4(1):124–132
2. Lewis BG, Paine DC (2000) Applications and processing of transparent conducting oxides. MRS Bull 25(8):22–27
3. Ren YH, Li CF, Li W et al (2019) Study on micro-grinding quality in micro-grinding tool for single crystal silicon. J Manuf Process 42246–42256
4. Aurich JC, Carrella M, Walk M (2015) Micro grinding with ultra small micro pencil grinding tools using an integrated machine tool. CIRP Ann 64(1):325–328
5. Walk M, Aurich JC (2014) Integrated desktop machine tool for manufacturing and application of ultra-small micro pencil grinding tools. Procedia CIRP 14333–14338
6. Yang YY, Yang M, Li CH et al (2023) Machinability of ultrasonic vibration-assisted micro-grinding in biological bone using nanolubricant. Front Mech Eng 18(1)
7. Perveen A, Wong YS, Rahman M (2011) Characterisation and online monitoring of wear behaviour of on-machine fabricated PCD micro-tool while vertical micro-grinding of BK7 glass. Int J Abras Technol 4(4):304–324
8. Cheng J, Gong YD, Wu ZZ et al Surface quality effects investigation of micro-grinding soda-lime glass; proceedings of the International Conference on Mechatronics and Materials Engineering (ICMME 2012), 2012.Hangzhou, PEOPLES R CHINA, F Jul 13–14, 2013
9. Cheng J, Gong YD, Wang JS (2013) Modeling and evaluating of Surface Roughness Prediction in Micro-grinding on Soda-lime glass considering Tool characterization. Chin J Mech Eng 26(6):1091–1100
10. Cheng J, Gong YD (2014) Experimental study of surface generation and force modeling in micro-grinding of single crystal

silicon considering crystallographic effects. International Journal of Machine Tools & Manufacture 771 – 15
11. Feng J, Chen P, Ni J (2012) Prediction of surface generation in microgrinding of ceramic materials by coupled trajectory and finite element analysis. Finite Elem Anal Des 5767–5780
12. Manea H, Cheng X, Ling SY et al (2020) Model for predicting the micro-grinding force of K9 glass based on material removal mechanisms. Micromachines 11(11)
13. Kubohori T, Inui Y, Ikuta T (2007) Evaluation of grinding characteristics of thermal spraying ceramics film. Mater Trans 48(5):1050–1054
14. Katahira K, Ohmori H, Komotori J et al (2010) Modification of surface properties on a nitride based coating films through mirror-quality finish grinding. CIRP Ann Manuf Technol 59(1):593–596
15. Masoumi H, Safavi SM, Salehi M (2014) Grinding force, Specific Energy and material removal mechanism in grinding of HVOF-Sprayed WC-Co-Cr coating. Mater Manuf Processes 29(3):321–330
16. Zoei MS, Sadeghi MH, Salehi M (2016) Effect of grinding parameters on the wear resistance and residual stress of HVOF-deposited WC-10Co-4Cr coating. Surf Coat Technol 307886–307891
17. Kar S, Bandyopadhyay PP, Paul S (2016) Precision superabrasive grinding of plasma sprayed ceramic coatings. Ceram Int 42(16):19302–19319
18. Kar S, Paul S, Bandyopadhyay PP (2016) Processing and characterisation of plasma sprayed oxides: microstructure, phases and residual stress. Surf Coat Technol 304364–304374
19. Kar S, Kumar S, Bandyopadhyay PP et al (2020) Grinding of hard and brittle ceramic coatings: force analysis. J Eur Ceram Soc 40(4):1453–1461
20. Qiu Y, Jin YL, Zhao H et al (2014) Physical properties of ITO thin films prepared by ion-assisted electron beam evaporation; proceedings of the International Symposium on Optoelectronic Technology and Application (IPTA) - Laser Materials Processing; and Micro/Nano Technologies, 2014.Beijing, PEOPLES R CHINA, F May 13–15
21. Lee KY, Choi GW, Kim YJ et al (2012) Chemical Mechanical polishing characteristics of ITO Thin Film prepared by RF Magnetron Sputtering. J Korean Phys Soc 60(3):388–392
22. Ziaei S, Wu Q, Fitch J et al (2019) Channel cracking and Interfacial Delamination of Indium Tin Oxide (ITO) Nano-Sized films on Polyethylene Terephthalate (PET) substrates: experiments and modeling. Exp Mech 59(5):703–712
23. Wang ZX, Wang SB, Wang JR et al (2021) Mechanical performance of ITO/Ag/ITO multilayer films deposited on glass substrate by RF and DC Magnetron sputtering. Ceram Int 47(22):31442–31450
24. Wan L, Li L, Deng Z et al (2019) Thermal-mechanical coupling simulation and experimental research on the grinding of zirconia ceramics. J Manuf Process 4741–4751
25. Huang S, Gao S, Huang C et al (2022) Nanoscale removal mechanisms in abrasive machining of brittle solids. Diam &Abrasives Eng 42(03):257–267
26. Qu SS, Wei CX, Yang YY et al (2024) Grinding mechanism and surface quality evaluation strategy of single crystal 4H-SiC. Tribol Int 194:109515
27. Zhang CY, Guo B, Zhao QL et al (2019) Ultra-precision grinding of AlON ceramics: surface finish and mechanisms. J Eur Ceram Soc 39(13):3668–3676
28. Zhang Q, To S, Zhao Q et al (2016) Surface generation mechanism of WC/Co and RB-SiC/Si composites under high spindle speed grinding (HSSG). Int J Refract Met Hard Mater 56123–56131
29. Tian L, Fu Y, Xu J et al (2015) The influence of speed on material removal mechanism in high speed grinding with single grit. Int J Mach Tools Manuf 89192–89201
30. Sun Y, Su ZP, Gong YD et al (2020) An experimental and numerical study of micro-grinding force and performance of sapphire using novel structured micro abrasive tool. Int J Mech Sci 181
31. Zhang XH, Kang ZX, Li S et al (2019) Grinding force modelling for ductile-brittle transition in laser macro-micro-structured grinding of zirconia ceramics. Ceram Int 45(15):18487–18500
32. Bifano TG, Dow TA, Scattergood RO (1991) Ductile-Regime Grinding: a New Technology for Machining Brittle materials. J Eng Ind 113(2):184–189
33. Ma LJ, Yu AB, Gu LC et al (2017) Mechanism of compound fracture and removal in grinding process for low-expansion glass ceramics. Int J Adv Manuf Technol 91(5–8):2303–2313
34. Piao YC, Li C, Hu YX, Cui HL, Luo XC, Geng YQ, Zhang FH (2024) Nanoindentation induced anisotropy of deformation and damage behaviors of MgF2 crystals. J Mater Res Technol 28:4615–4625
35. Liu Y, Li J, Zhao Z et al (2024) Advanced grinding technologies for silicon carbide ceramic: a review. J Adv Manuf Sci Technol 4(1):2023016
36. Qu SS, Yao P, Gong YD et al (2022) Modelling and grinding characteristics of unidirectional C-SiCs. Ceram Int 48(6):8314–8324
37. Hsu J-S, Lee C-C, Wen B-J et al (2016) Experimental and simulated investigations of thin polymer substrates with an Indium Tin Oxide Coating under fatigue bending loadings. Materials 9(9):720
38. Jung HS, Eun K, Kim YT et al (2017) Experimental and numerical investigation of flexibility of ITO electrode for application in flexible electronic devices. Microsyst Technologies-Micro-and Nanosystems-Information Storage Process Syst 23(6):1961–1970
39. Lv B, Lin B, Cao Z et al (2024) Damage and crack extension mechanism of hard and brittle materials induced by cyclic indentation. J Adv Manuf Sci Technol 4(2):2024003
40. Li C, Hu YX, Wei ZZ, Wu CJ, Peng YF, Zhang FH, Geng YQ (2024) Damage evolution and removal behaviors of GaN crystals involved in double-grits grinding. Int J Extreme Manuf. https://doi.org/10.1088/2631-7990/ad207f
41. Wu M, Wang C, Zheng L et al (2022) Research on grinding of biological tissue. Diam Abrasives Eng 42(2):137–149
42. Zhang JH, Li H, Zhang ML et al (2017) Study on force modeling considering size effect in ultrasonic-assisted micro-end grinding of silica glass and Al_2O_3 ceramic. Int J Adv Manuf Technol 89(1–4):1173–1192
43. Qu SS, Yao P, Gong YD et al (2022) Environmentally friendly grinding of C/SiCs using carbon nanofluid minimum quantity lubrication technology. J Clean Prod 366:132898
44. Yang YY, Gong YD, Li CH et al (2021) Mechanical performance of 316 L stainless steel by hybrid directed energy deposition and thermal milling process. J Mater Process Technol 291:117023

Publisher's Note Springer Nature remains neutral with regard to jurisdictional claims in published maps and institutional affiliations.

Springer Nature or its licensor (e.g. a society or other partner) holds exclusive rights to this article under a publishing agreement with the author(s) or other rightsholder(s); author self-archiving of the accepted manuscript version of this article is solely governed by the terms of such publishing agreement and applicable law.